RIBBON GROWTH ON SUBSTRATE - A ROADMAP TO HIGHER EFFICIENCIES

S. Seren[1], G. Hahn[1], A. Gutjahr[2], A. R. Burgers[2], A. Schönecker[2]
[1] University of Konstanz, Department of Physics, 78457 Konstanz, Germany
[2] ECN - Solar Energy, P.O. Box 1, 1755 ZG Petten, Netherlands

ABSTRACT: Ribbon Growth on Substrate (RGS) is a very promising low cost silicon ribbon material for photovoltaics. The RGS production principle allows the direct growth of silicon wafers ready for solar cell processing without any aftertreatment such as wiresawing with a very high production speed of one wafer per second. The material quality of the wafers was continuously improved during the last years in terms of a lowered oxygen content. The lowered oxygen content allows a faster hydrogen diffusion which enables an enhanced passivation of bulk defects. As a result the lifetime of the RGS material strongly improved and shows average values of up to 5 µs on present material within an industial type screen-printing firing through silicon nitride solar cell process. Until a new, totally rebuilt production facility is finalized, which is currently built up, the efficiencies of RGS solar cells can be improved by different process related approaches such as gettering of impurities, hydrogenation of bulk defects, avoidance of material and process induced shunts as well as surface texturisation. A further basic approach is to utilize the occuring drift field of gallium doped RGS wafers in order to enhance J_{sc}. Due to the fine crystal structure of RGS material with crystal sizes in the submillimeter range different surface texturisation methods had to be analysed. Reflectivity and quantum efficiency measurements demonstrate the achievable gain in J_{sc}. Because of the limited output of the lab-scale R&D machine solar cell processing was performed on 5x5 cm^2 wafers in the past and resulted in cell efficiencies close to 13%. 12% efficient 10x10 cm^2 RGS solar cells are presented and demonstrate the scalability of both the material homogeneity and the cell process.

Keywords: Ribbon Silicon, Passivation

1 INTRODUCTION

This paper focuses on a very promising silicon ribbon material currently produced for research: Ribbon Growth on Substrate (RGS [1,2]) by ECN. The material is investigated in terms of solar cell processing and characterisation. Because of the material production principle the throughput is very high compared to other silicon ribbon materials like String Ribbon or EFG [3]. As a consequence the crystal quality suffers from higher crystal defect densities such as dislocations, grain boundaries or impurities incorporated by the crucible, casting and substrate material which limits the lifetime of the material. To overcome this limitation the applied adapted industrial type screen printing process has to ensure a sufficient bulk hydrogenation and the avoidance of material and process induced shunts. The wafer size is scalable in a wide range up to 6 square inches limited only by the substrate sizes used. First cell results of untextured large area 10x10 cm^2 RGS cells are presented as well as results from untextured 5x5 cm^2 cells. Due to the discontinuously, not in thermal equilibrium working lab-scale R&D RGS machine the space for further major improvements of the as grown RGS material is limited. This situation will change once the continuously operating RGS production machine will be in operation in 2007. Thus in order to increase J_{sc} of solar cells processed from RGS material of the current material quality different texturisation methods were analysed as well as an occuring drift field in Ga doped wafers.

2 SHUNTING IN LOW [O_i] RGS

Shunting in low [O_i] RGS was observed in the past [4,5,6,7,8]. There are different shunting mechanisms possible such as current collecting channels (only occuring in older high [O_i] RGS material [9]), cracks and micro defects originating from the rapid crystal growth and the subsequent planarisation of the uneven wafer surface, inhomogeneities in the emitter formation due to enhanced emitter diffusion along grain boundaries [10], aluminium reaching the solar cell front side during the alloying process of the back contact formation [8] through cracks, holes or extended crystal defects. Carbon related precipitates penetrating the space charge region are expected to be responsible especially for observed areal shunts due to a carbon concentration of the RGS material above the carbon solubility limit [4].
To avoid or at least to reduce process induced shunts the following experiment was performed to clarify the origin of the observed strong point shunts. A RGS wafer was planarised using a convertional wafer dicing saw and an acidic saw damage etch was performed in order to remove the defect rich surface layer induced by the planarisation step. A $POCl_3$ emitter diffusion (50 Ω/sq.) followed with a subsequent removal of the P-glass. To check if enhanced emitter diffusion along defects or grain boundaries caused shunting an, illuminated Lock-In Thermography (iLIT [11]) shunt scan was performed (Figure 1, left).

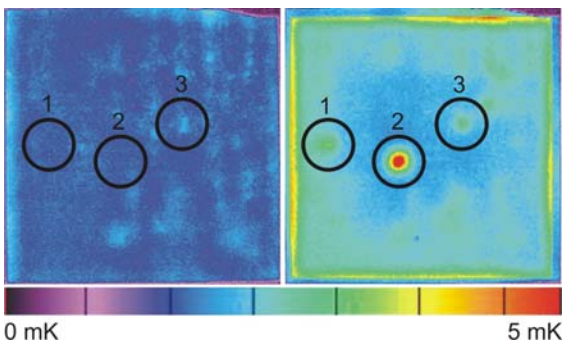

Figure 1: iLIT measurement of a wafer after $POCl_3$ emitter diffusion (left) and subsequent screen printing and firing of a fully covering aluminium backside metallisation (right). Same scaling for both images. The strong point shunt (3) is formed during the aluminium alloying process.

Figure 1 reveals that some minor (rather areal) shunts are induced by the phosphorous diffusion. A screen printing of a full covering aluminium back contact and alloying at standard firing conditions and subsequent iLIT measurement revealed that the heavy point shunt shown in Figure 1 (right, shunt number 2) is formed during the alloying process. There are two possibilities for the origin of that particular shunt. To check if aluminium was soaked via extended defects (cracks or holes) through the entire wafer to the wafer front side or if a phosphorous channel deep in the wafer is in electrical contact with the aluminium backside metallisation, the shunted part of the wafer was analysed using scanning electron microscopy and Energy Dispersive X-Ray Spectroscopy (EDX). On the wafer front surface at the position of the shunt (Figure 1, shunt number 2) aluminium could be identified which gives a clear evidence that aluminium was soaked through the entire wafer to the wafer front surface during the alloying process.

Figure 2: Electron microscopy of the shunted part of the wafer shown in Figure 1 (left). EDX scans of this region (Figure 3) identified the shown formations as aluminium.

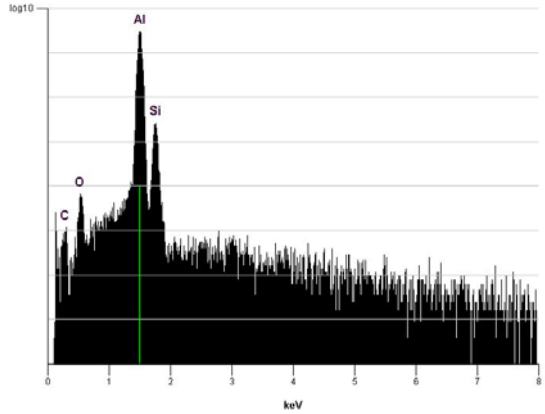

Figure 3: EDX scan of the shunted part of the wafer shown in Figure 1 and Figure 2.

The other weaker shunts shown in Figure 1 originate most probably from similar mechanisms. Shunt number 3 suggests an extended phosphorpos diffusion along grain boundaries or extended defects. The heat dissipation of this shunt is enhanced after aluminium alloying which can be explained by a contact formation of aluminium and the shunted region during alloying. Shunt number 1 marked in Figure 1 forms not until aluminium alloying.

Thus a single side emitter diffusion was chosen for the following solar cell processes in order to reduce the extended phosporous diffusion along grain boundaries and extended defects. Further on, an open rear side metallisation (grid [7,8]) was chosen for the cell process described in the following to reduce the probability of contacting the emitter and to alloy aluminium at areas where the wafer suffers from extended defects.

3 CELL PROCESS AND LIFETIME

RGS wafers are currently produced by a laboratory scale R&D machine at ECN and cells reported here were processed at the University of Konstanz (UKN) according to an industrial type screen printing process shown in Figure 4. Due to occurance of shunting in low $[O_i]$ RGS material, a single side emitter open rear side process with an aluminium coverage of the rear of 10% was used.

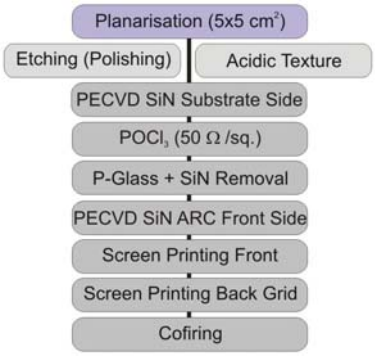

Figure 4: Shunt avoiding open rear side (10% coverage) screen printing process. The applying of a texture is optional.

During $POCl_3$ emitter diffusion and cofiring of the metallisation phosphorus respectively aluminium gettering takes place as well as a hydrogenation of bulk defects by hydrogen originating from the hydrogen rich SiN antireflective coating. As a result the minority carrier lifetime is strongly enhanced. Figure 5 shows spatially resolved lifetime measurements (µPCD in low injection) of an as grown wafer and a wafer originating from the same RGS production run after cell processing and subsequent removal of the metal contacts, SiN antireflective coating and emitter. The wafer surfaces were passivated using iodine/ethanol for both measurements. The average as grown lifetime of 0.5 µs is enhanced by a factor of 10 to 5 µs during the applied solar cell process.

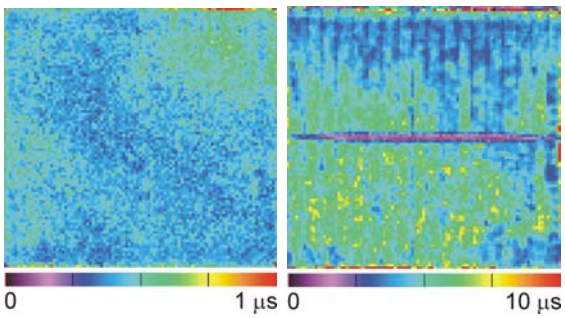

Figure 5: Spatially resolved lifetime measurements (µPCD) of RGS wafers. Left: as grown. Right: after solar cell processing and etching off metallisation, antireflective coating and emitter. The two 5x5 cm^2 wafers originate from the same RGS production run.

4 SURFACE TEXTURISATION

To enhance J_{sc} different surface texturisation methods were tested on RGS material. Two different Isotextures and a Pyramid texture were applied: Isotexture 1 [12] (isotropic acidic, HNO_3, HF, H_2O), developed at UKN, Isotexture 2 (isotropic acidic, H_2SO_4, HF, HNO_3) and a Pyramid texture (anisotropic alkaline), developed at UKN.

Figure 6 shows the reflection curves of an untextured (polishing etched) and differently textured RGS wafers without applying an antireflective coating. Isotexture 1 shows the lowest reflection over the entire wavelength range.

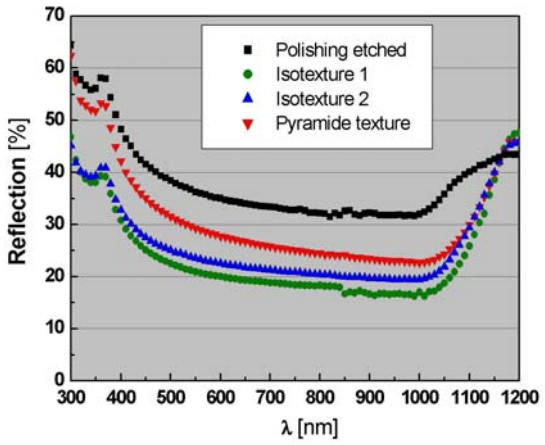

Figure 6: Reflection curves of polishing etched and textured RGS material without an antireflective coating using different texturisation methods. Applying Isotexture 1 results in the lowest overall reflection. A similarly low reflection is achieved by applying Isotexture 2.

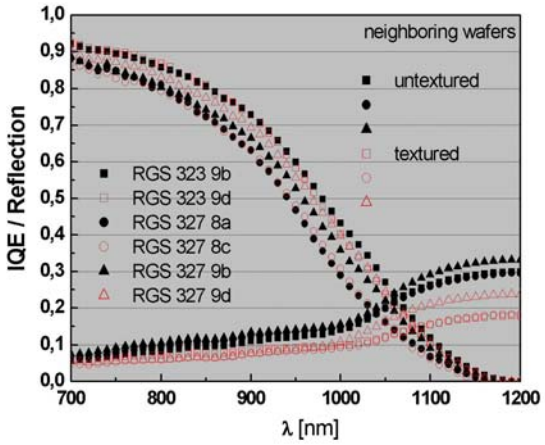

Figure 7: IQE and reflection data of solar cells originating from neighboring RGS wafers (5x5 cm^2 cells originate from the same 12x8 cm^2 RGS wafer). The IQEs of the textured cells (Isotexture 2) show a slight enhancement in the long wavelength range due to a better light trapping.

Isotexture 2 was tested on RGS solar cells (Figure 7) and resulted in a gain in J_{sc} of up to 1.1 mA/cm^2. Isotexture 1 and the Pyramid texture were tested within the RGS screen printing process as well. Due to a deeper surface damage on RGS wafers compared to standard multicrystalline wafers (average saw damage depth of 15 µm) the surface damage removal by acidic etching and the subsequent texturisation have to be adjusted exactly.

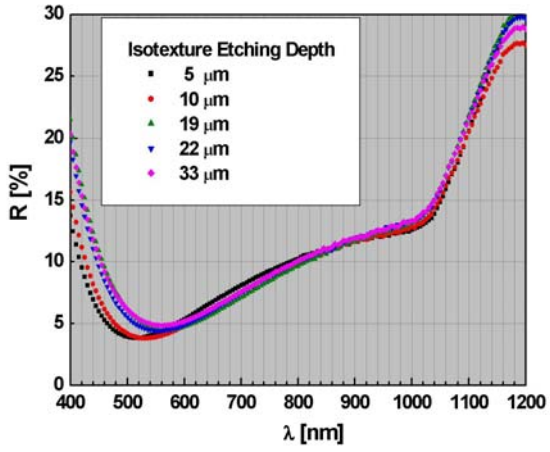

Figure 8: Reflection data of textured solar cells (Isotexture 1 and antireflective coating) with different etching depths. The smallest etching depth (5 µm) results in the best reflection.

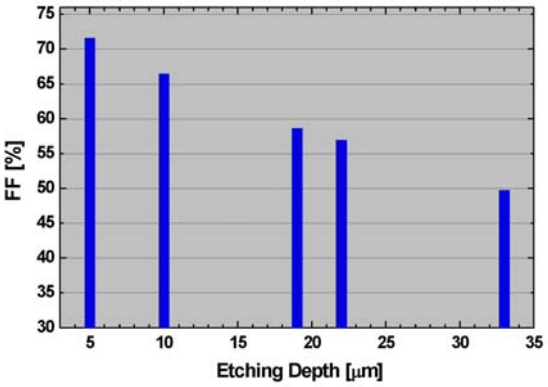

Figure 9: Fill Factors of the same textured solar cells as shown in Figure 8. The smallest etching depth (5 µm) results in the best reflection and the best FF.

Figure 9 shows FFs of solar cells processed from RGS wafers originating from the same RGS production run. After planarising the uneven wafer surfaces and thus the generation of a damaged wafer surface (comparable to the saw damage of standard mc wafer material) Isotexture 1 was applied for different durations resulting in etching depths from 5 to 33 µm. The Isotexture 1 solution works only if a saw damage is present thus only the planarised wafer front side was etched. The unplanarised wafer substrate side remains almost untouched. Although Isotexture 1 was developed for multicristalline materials with an isotropic etching characteristic, the FFs shown in Figure 9 suffer from prolonged etching. RGS material with grain sizes below 1 mm contains much more grain boundaries compared to standard mc material. Thus due to an enhanced etching rate of the texture solution at grain boundaries the etching depth is strongly increased at grain boundaries for longer etching durations. The loss in FF for prolonged etching depths correlates with lowered parallel resistances shown in Figure 10 due to an enhanced $POCl_3$ emitter diffusion at the deeper etched grain boundaries.

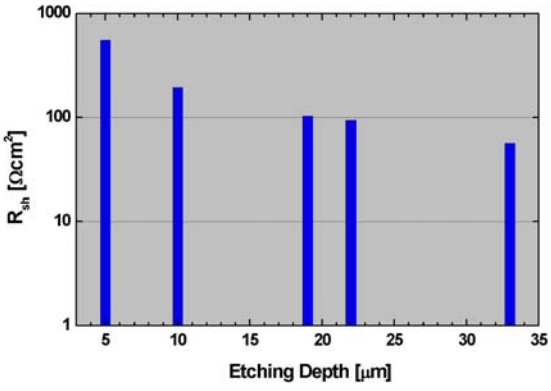

Figure 10: Parallel resistances of the same textured solar cells as shown in Figure 8 and 9. The best parallel resistance is obtained for the lowest etching depth.

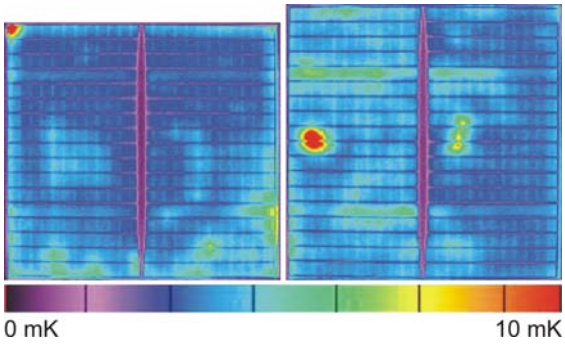

Figure 11: iLIT measurement of two textured (Isotexture 1) RGS solar cells. Same scaling for both cells. Texture depth left 10 µm, right 33 µm. The amount and the strength of shunts (red dots and light areas) can be correlated with the shunt values given in Figure 10.

Besides the reduction in FF with prolonged etching depth textured (Isotexure 1) RGS solar cells show an average enhancement in J_{sc} of 1.4 mA/cm^2 compared to RGS solar cells processed within the same experiment but without applying the texture.

The Pyramid texture (reflection curve shown in Figure 6) shows a similar behaviour in terms of reduced FFs with prolonged etching depths as well due to an enhanced etching of grain boundaries.

Although enhanced J_{sc} values are measured for textured RGS solar cells (Isotexture 1, Isotexture 2 and Pyramid texture) no enhancement in efficiency could be reached so far due to the accompanied reduction in FF with texturing. Further on the anyway necessary planarisation of the uneven RGS wafer surface applies a mechanical microtexture which reduces the overall reflection of the planarised wafers compared to untextured standard mc wafers. Thus the reflection of RGS solar cells processed according to the screen printing process presented above reduces the reflection of the RGS material without reducing the FF. J_{sc} values of the best untextured RGS solar cells reached 29 mA/cm^2 compared to the best textured (Isotexture 1 as well as Isotexture 2) RGS solar cells wich reached a maximum in J_{sc} of 29.5 mA/cm^2.

5 CELL RESULTS

Table I: IV data of three of the best screen-printed RGS cells (SiN single layer ARC) from low [O_i] RGS processed at UKN.

screen printed RGS cell	V_{oc} [mV]	J_{sc} [mA/cm^2]	FF [%]	η [%]
low [O_i] untextured (completely covered rear side)				
4.9x4.9 cm^2	580	28.1	75.6	12.3
low [O_i] untextured (completely covered rear side)				
9.8x9.8 cm^2	574	27.9	74.3	11.9
low [O_i] untextured (single side emitter, open rear side)				
5x5 cm^2	590	29.4	75.1	13.0

The best 5x5 cm^2 cell processed at the UKN from low [O_i] RGS material achieved an efficiency of 13% (not yet independently confirmed), the best confirmed RGS cell 12.3%. This result was confirmed by a

measurement at an ISO 17025 accredited calibration laboratory, namely the European Solar Test Installation (ESTI) of the Joint Research Centre (JRC) of the European Commission. Approximately the same efficiency could be achieved on a large 10x10 cm^2 RGS wafer which demonstrates the scalability of the material quality and the solar cell process.

Due to the rapid crystal growth of the RGS wafer material and the direct contact of the wafer with the substrate material during crystallisation, the crystal growth velocity is determined by the heat transport in the substrate material through the already solidified wafer fraction. Thus the crystal growth velocity is nonlinear and depends besides other parameters on the thickness of the finished wafer. Figure 12 shows an iLIT measurement of the 10x10 cm^2 solar cell presented in Table I. Although the cell was processed from a relatively thin (approx. 200 µm) RGS wafer using a double side emitter diffusion and a fully covering aluminium back contact, very low shunting is visible. Crystallographic investigations gave hints for a more disturbed crystal structure during the growth of thicker RGS wafers.

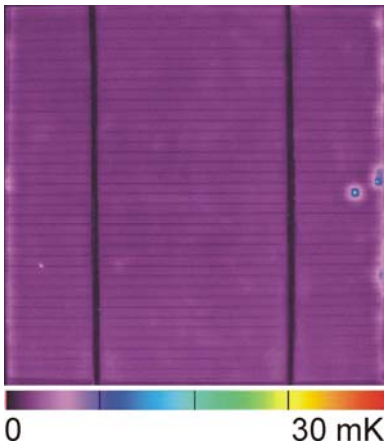

Figure 12: iLIT measurement of a 10x10 cm^2 RGS solar cell. Except a few small edge shunts on the right cell edge the cell is free of shunts.

6 DRIFT CELL

Ga doped RGS wafers were produced by ECN as well. Ga as a dopant has the advantage to avoid recombination active boron-oxygen complexes degrading lifetimes. On the other hand Ga as a dopant in the RGS process results in a depth dependent dopant concentration in the wafers. This is a well known effect due to the low segregation coefficient for Ga in Si (k = 0.008) for low crystal growth velocities and has been applied e.g. to the EFG material in the past [13]. Opposite to almost steady state crystallisation, the RGS process is characterised by rapidly changing crystallisation speed with growing thickness of the wafer [14]. The initial high growth velocity results in k_{eff} close to unity at the beginning of wafer crystallisation. As crystal growth velocity decreases with increasing wafer thickness, segregation becomes more effective. By controlling the thermal properties of the RGS wafer crystallisation, a gradient in dopant concentration throughout the wafer thickness can be achieved, enhancing the minority carrier transport towards the pn-junction by a drift field [15]. Such a doping gradient could be measured on a Ga doped RGS wafer [6] using ECV. In order to analyse the drift field RGS wafers with different overall Ga doping concentrations were processed using the screen printing process described above. Half of the wafers were processed with the emitter on the free wafer surface, the other half with the emitter on the wafer substrate side.

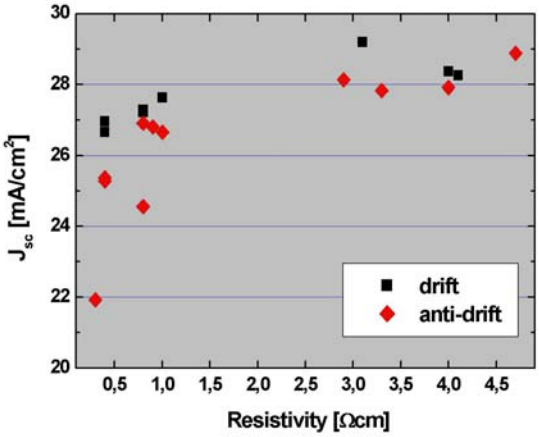

Figure 13: J_{sc} values of RGS solar cells containing different overall Ga doping concentrations processed with the emitter on the free wafer surface (drift) and the emitter on the wafer substrate side (anti-drift).

A clear tendency of lowerd J_{sc} values for the anti-drift cells with a higher overall doping concentration is found as a result of the inhomogeneous bulk doping (drift field). It is suggested that the field ranges through the entire wafer pointing from lower to higher doping concentrations (i.e from the free wafer surface to the wafer substrate side). Minority charge carriers (electrons) would follow the drift field in opposite direction resulting in an enhanced J_{sc} of the processed drift-cells. The anti-drift field on the other hand would hinder the minority charge carriers to drift to the pn-junction resulting in a lowered J_{sc} of the processed anti-drift cells. Figure 13 verifies the suggested correlation. Further on the drift effect is enhanced with higher doping concentrations (i.e. the difference in J_{sc} of drift and anti-drift cells) and a maximum in J_{sc} is found for 3 Ωcm material wich produces the best results for B doped material as well. The simulated efficiency gain of a solar cell with typical RGS material parameters and a linear doping concentration gradient in the order of the measured values is $0.5\%_{abs.}$ due to the enhanced J_{sc} as compared to a solar cell with a uniform bulk doping.

Table II: IV data of two of the best screen-printed Ga doped RGS cells (drift-cell) processed at the UKN according to the process described above.

screen printed RGS drift-cell	**V_{oc} [mV]**	**J_{sc} [mA/cm^2]**	**FF [%]**	**η [%]**
3 Ωcm material				
4.9x4.9 cm^2	581	29.5	68.1	11.7
0.5 Ωcm material				
4.9x4.9 cm^2	596	27.2	68.6	11.1

In addition Table II shows a V_{oc} of 596 mV on

0.5 Ωcm material which is the highest open circuit voltage reached on screen printed RGS solar cells. The FFs of the Ga doped RGS cells suffer from low shunt values which results in lowered V_{oc} values although the shunt reducing screen printing process described above was used. The origin of the low shunt values is unclear up to now and under investigation.

7 OUTLOOK

The most limiting factor for higher efficiencies for solar cells processed from actual RGS material from the laboratory scale R&D machine are reduced fill factors due to shunting occuring in low [O_i] RGS material. Efficiencies well above 13% should easily be reachable as soon as these material induced shunts can be avoided. One approach hereby is to reduce the carbon concentration in RGS wafer material by using optimised casting and substrate materials. 10x10 cm^2 RGS solar cells with very low shunting processed from thin wafer material suggest that shunting may be reduced by growing thinner RGS wafers which is done currently. First thin screen printed RGS solar cells (thickness approx. 100 µm) were processed without planarising the wafer surface and reached an efficiency of 10.6%. By optimizing surface texturisation methods on RGS material J_{sc} should be enhanced further on without limiting the FFs of the textured solar cells. Another approach to enhance cell efficiency is to utilize n-type RGS material which is currently produced and investigated. The most significant enhancement in material quality is expected to result from a new, totally rebuilt production facility operating continuously in thermal equilibrium which is built up currently.

8 SUMMARY

RGS material is produced within a horizontal crystal growth configuration and shows a high crystal growth velocity resulting in a fine grain structure and therefore a limited diffusion length. This limitation could be enhanced significantly by gettering and hydrogenation during cell processing within an industrial type screen printing firing through SiN process. Lifetime measurements performed on as grown (0.5 µs) and processed (5 µs) RGS material show an enhancement in lifetime by a factor of 10. Shunting occuring in low [O_i] RGS material can be avoided by using a single side emitter formation and an open rear side metallisation with 10% coverage.

The origin of strong point shunts could be identified as aluminium penetrating the entire wafer thickness during alloying of the backside metallisation using Lock-In Thermography (iLIT) in combination with scanning electron microscopy (EDX).

In order to enhance J_{sc} different surface textures were tested resulting in an average gain in J_{sc} of 1.4 mA/cm^2.

Solar cell efficiencies of 12.7% for 5x5cm^2 as well as 12% for 10x10cm^2 showed the scalability of the material and the applied solar cell process. Further on iLIT measurements revealed very low shunting in solar cells processed from thinner RGS material. First unplanarised RGS wafers with a thickness of approx. 100 µm were processed (screen printing) and reached an efficiency of 10.6%.

Ga doped drift cells were processed and showed a doping concentration dependant enhancement in J_{sc} of up to 0.5 mA/cm^2 due to a built in drift field but limited FFs.

9 ACKNOWLEDGEMENTS

Part of this work was funded by the EC in the RGSells project (ENK6-CT-2001-00574). The RGS wafer manufacturing process development is carried out in the RGSolar project supported by the Dutch EET programme under EETK 03023.

10 REFERENCES

[1] H. Lange, I. A. Schwirtlich, Ribbon Growth on Substrate (RGS) - A new approach to high speed growth of silicon ribbons for photovoltaics, J. Cryst. Growth, 104 (1990) 108

[2] G. Hahn, A. Schönecker, New crystalline silicon ribbon materials for photovoltaics, J. Phys.: Condens. Matter 16 (2004) R1615-R1648

[3] M. J. Kardauskas, M. D. Rosenblum, B. H. Mackintosh, J. P. Kalejs, The coming of age of a new PV wafer technology – some aspects of EFG polycristalline silicon sheet manufacture, Proc. 25th IEEE PVSEC, Washington D.C. 1996

[4] S. Seren, G. Hahn, A. Gutjahr, A. R. Burgers, A. Schönecker, Screen-Printed Ribbon Growth on Substrate Solar Cells approaching 12% Efficiency, 31th IEEE PVSEC; Florida 2005

[5] S. Seren, G. Hahn, A. Gutjahr, A. Burgers, A. Schönecker, A. Grenko, R. Jonczyk, Ribbon Growth on Substrate and Molded Wafer - Two low cost silicon ribbon materials for PV, submitted to the 4th WCPEC, Waikoloa 2006

[6] S. Seren, G. Hahn, F. Huster, R. Kopecek, A. Gutjahr, A. R. Burgers, A. Schönecker, Screen-printed Ribbon Growth on Substrate Solar Cells exceeding 12% Efficiency, 20th EC PVSEC, Barcelona 2005

[7] A. Burgers, A. Gutjahr, L. Laas, A. Schönecker, S. Seren, G. Hahn, Shunt free solar cells on RGS wafers, 4th WCPEC, Waikoloa 2006

[8] A. Burgers, S. Seren, A. Gutjahr, A. Schönecker, G. Hahn, Record 12.9% efficiency screen printed silicon solar cells on RGS material, 21st EPSEC, Dresden 2006

[9] G. Hahn, C. Haessler, M. Langenkamp, 12.5% efficient RGS silicon solar cells with carrier collecting channels, 16th EC PVSEC, Munich 2001

[10] P. Holloway, T. Abrantes, Grain boundary diffusion of phosphorous in silicon, J. Vac. Sci. Technol, 7 (1989) 1573-8

[11] M. Kaes, S. Seren, T. Pernau, LimoLIT – A novel Thermographic Characterisation Method for p/n Structures and Solar Cells, Proc. 19th EC PVSEC, Paris 2004

[12] A. Hauser, I. Melnyk, E. Wefringhaus, F. Delahaye,

G. Vilsmeier, P. Fath, Acidic Texturisation of mc-Si using a high Throughput In-Line Prototype System with no Organic Chemistry, 19th EC PVSEC, Paris 2004

[13] R. O. Bell et al, 18th IEEE PVSC, Las Vegas 1985, 764

[14] A. Schönecker et al, 12th NREL workshop on silicon solar cell materials, Breckenridge 2002, 7

[15] Patent pending.